2nd IFAC Workshop on Automatic Control in Offshore Oil and Gas Production,
May 27-29, 2015, Florianópolis, Brazil

Modal Reduction Based Tracking Control for Installation of Subsea Equipments ⋆

Fabricio Rodrigues Monteiro *
Jose Oniram de Aquino Limaverde Filho *
Eugenio Fortaleza *

* *GRACO - Grupo de Automação e Controle, Universidade de Brasilia, Brasilia, Brazil, (e-mail: fabriciorm9@gmail.com, joseoniram@ieee.org, efortaleza@unb.br)*

Abstract: This paper proposes a control strategy for the deep sea installation of wellhead equipments hanged by flow line structures, named risers. A fundamental step of this operation is the positioning of the equipment over the wellhead, which can be costly, time-consuming, and unfeasible in bad weather conditions. The approach taken considers the riser structure an Euler-Bernoulli beam submerged in a fluid, whose top end is fixed in the offshore platform and the bottom end attached to a payload. A dynamic analysis is carried to identify the structure's most significant modes of vibration and create a reduced-order model. Then, a flatness-based approach is used for trajectory planning and tracking, resulting in a low complexity control structure. Numerical simulations are presented to validate the proposed controller and to analyse its performance in the presence of external perturbations.

Keywords: Offshore Structures, Distributed Parameter Systems, Modal Reduction, Trajectory Tracking.

1. INTRODUCTION

Deep sea oil exploration is more and more common around the world, as oilfields onshore and in shallow waters become scarce and insufficient for the current demand. Many technological challenges in the *Exploration & Production* (E&P) sector appear from the rough conditions in deep sea.

Due to the depth, fixed platforms are substituted by floating and mobile ones, requiring the transposition of essential wellhead equipments from the surface to the seabed, like the Blow-Out Preventer (BOP), during drilling, and the Christmas Tree (X-Mas Tree), after completion. In this context, the external loads caused by waves and marine currents induce motion and vortex-induced vibrations (VIV) on the riser structures, leading to complex behavior. Analysis and control for these structures have been motivated as a means to reduce operation times, fatigue, and avoid collisions between them.

Yamamoto et al. (2007) proposes a linear quadratic regulator (LQR) to include the riser dynamics in a semi-submersible platform control system. Ioki et al. (2006) focus on the non-linear hydrodynamical forces on the riser to propose a linear parameter varying (LPV) control. In Fortaleza et al. (2011), a flat simplified model is developed and used for trajectory tracking by two different approaches: Lyapunov analysis and model inversion.

⋆ The authors would like to to acknowledge the Brazilian institutions: ANP, FINEP-MCT, and Petrobras for supporting the present study and PRH-PB 223.

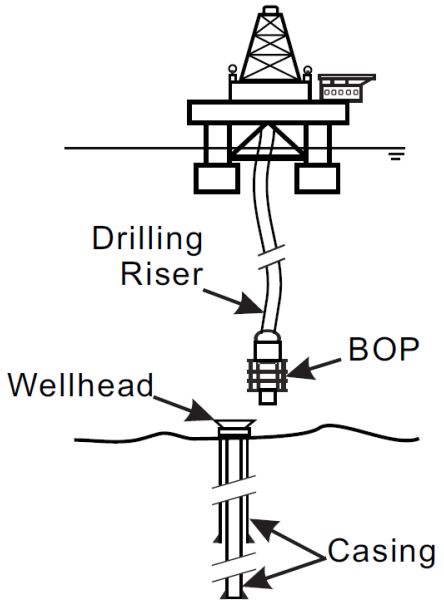

Fig. 1. Reentry operation (Fortaleza et al. (2012))

In this paper it is proposed a control strategy for the installation of the BOP hanged by the drilling riser, called reentry operation (see Fig. 1). For that, we make use of flatness, a property observed in some dynamical systems that allows the trivialization of trajectory planning and tracking. This property allows a complete parametrization of all systems variables (states, inputs, outputs) in terms of a finite set of independent variables, called the flat outputs,

and a finite number of their time derivatives. See Sira-Ramirez and Agrawal (2004).

In addition, a reduced-order model is developed to represent the original riser system, according to Fortaleza (2009) and Sabri (2004). The novel approach consists in combining flatness with state estimation and prediction to design trajectory planning and tracking control laws. Initially, the flat output of the reduced system is used to find the desired open loop trajectories for the input and state variables of the system, given an arbitrary planned trajectory for the riser bottom end. A closed loop control law is obtained by an equivalent linear controllable system in Brunovsky's canonical form, whose state variables are the flat output and its time derivatives.

For trajectory tracking, the controller relies on full state estimation for the reduced model, given by an implemented standard Kalman filter. In addition, increased performance is achieved with a smith predictor in the control loop. Numerical simulations were carried out to test the robustness and performance of the controller under environmental perturbations.

2. GOVERNING EQUATIONS

Subsea structures like risers are slender and have a high shear modulus. Therefore, the Euler-Bernoulli beam simplification is used for modeling purposes. Equation (1) represents the horizontal displacement $\Upsilon(z,t)$ of the beam under external hydrodynamic forces and traction:

$$m_s \frac{\partial^2 \Upsilon}{\partial t^2} = -EJ \frac{\partial^4 \Upsilon}{\partial z^4} + \frac{\partial}{\partial z}\left(T(z)\frac{\partial \Upsilon}{\partial z}\right) + F_n(z,t) \quad (1)$$

where m_s is the linear density, E the Young's modulus, and J the second moment of area of the riser. $T(z)$ describes the tractive forces along the riser's length. $F_n(z,t)$ is the resultant external force.

The only external forces acting on the riser are hydrodynamic, except on its top and bottom ends, where reaction forces follow boundary conditions. Morison's equation describes the resultant external force:

$$F_n(z,t) = -m_f \frac{\partial^2 \Upsilon}{\partial t^2} - \mu \left|\frac{\partial \Upsilon}{\partial t}\right| \frac{\partial \Upsilon}{\partial t} \quad (2)$$

with m_f as the added fluid mass and μ, the drag constant. Naming $m = m_s + m_f$ and substituting (2) in (1):

$$\frac{\partial^2 \Upsilon}{\partial t^2} = -\frac{EJ}{m}\frac{\partial^4 \Upsilon}{\partial z^4} + \frac{\partial}{\partial z}\left(\frac{T(z)}{m}\frac{\partial \Upsilon}{\partial z}\right) - \frac{\mu}{m}\left|\frac{\partial \Upsilon}{\partial t}\right| \frac{\partial \Upsilon}{\partial t} \quad (3)$$

Since the traction $T(z)$ is mostly due to the heavy payload, it can be assumed an average value T for it, taken in the middle of the riser's length. Also, an alternate equation comes from linearizing the drag term, by replacing $\frac{\mu}{m}\left|\frac{\partial \Upsilon}{\partial t}\right|$ by a constant τ that takes the mean value of $\left|\frac{\partial \Upsilon}{\partial t}\right|$ into account:

$$\frac{\partial^2 \Upsilon}{\partial t^2} = -\frac{EJ}{m}\frac{\partial^4 \Upsilon}{\partial z^4} + \frac{T}{m}\frac{\partial^2 \Upsilon}{\partial z^2} - \tau \frac{\partial \Upsilon}{\partial t} \quad (4)$$

The top end boundary conditions are $\Upsilon(L,t) = u(t)$ and $\frac{\partial \Upsilon}{\partial z}(L,t) = 0$ for a fixed end in which the input force $u(t)$ from the platform is applied. For the bottom payload end, $\frac{\partial \Upsilon}{\partial z}(0,t) = \frac{F_L}{T}$, with F_L being the force applied by the riser end on the payload.

2.1 Discretization

For the control design explored in this paper, the system must have a finite state space. Therefore, the finite differences method is applied to the spatial coordinate z, as a means to approximate the governing PDE (4) into a finite number of ODEs. Given a discretization element in position $k \in \mathbb{N} : 1 \leq k \leq N$, being N the number of discretization elements, (4) becomes

$$\begin{aligned}\frac{d^2 \Upsilon_k}{dt^2} = &-\frac{EJ}{ml^4}(\Upsilon_{k-2} - 4\Upsilon_{k-1} + 6\Upsilon_k - 4\Upsilon_{k+1} + \Upsilon_{k+2}) \\ &+ \frac{T_0}{ml^2}(\Upsilon_{k-1} - 2\Upsilon_k + \Upsilon_{k+1}) - \tau \frac{d\Upsilon_k}{dt}\end{aligned} \quad (5)$$

with l as the distance between two discretization points ($l = L/N$), L the length of the riser.

From equation (5), we can represent the original system in a linear state space form ($\dot{\mathbf{x}} = \mathbf{A}\mathbf{x} + \mathbf{B}u\ ,\ y = \mathbf{C}\mathbf{x}$), with

$$\begin{aligned} x &= \left(\Upsilon_1\ \Upsilon_2\ ...\ \Upsilon_N\ \dot{\Upsilon}_1\ \dot{\Upsilon}_2\ ...\ \dot{\Upsilon}_N\right)^T_{2N\times 1} \\ u &= \Upsilon(L,t) \\ y &= \Upsilon(0,t) \end{aligned} \quad (6)$$

The system order is $2N$, since the state variables in are the displacement and speed of each discretization element. The input u and output y correspond to the top and bottom displacements, respectively, as discussed in the last subsection. A high number of elements is necessary to a faithful approximation, and, therefore, the traditional tracking control structure is too computationally intense, due to the matrix operations, and unrealistic, for requiring sensors along all the length of the riser. Next section presents a reduced-order model as a solution.

3. A MODEL ORDER REDUCTION STRATEGY

Most of the classical control theory deals with systems represented by a small number of state variables. Hence, a way to apply classical control methods in the literature to discretized distributed parameter systems is through a model order reduction.

In this paper, this is performed in two stages: first, a modal transformation is applied in the original system space state equations, as described in Dahleh (2011), resulting in a new representation in modal variables. In this form, the system can be seen as a set of decoupled subsystems in parallel, whose influence in the complete output can be computed individually. Then, the subsystems with the highest static gains are chosen to create a reduced order model, as detailed by Fortaleza (2009).

3.1 Modal Decomposition

Given the riser system's state space, first find its eigenvalues. These are always distinct between each other, a

sufficient condition for the diagonalization of the system state matrix. Then, we compute the modal matrix $\mathbf{T}$, whose ith column is the ith eigenvector of the system:

$$\mathbf{T} = (\mathbf{v_1} \mid \mathbf{v_2} \mid \ldots \mid \mathbf{v_{2N}})_{1\times 2N} \tag{7}$$

Matrix $\mathbf{T}$ is used for a similarity transformation on the original system ($\mathbf{A_M} = \mathbf{T^{-1}AT}$, $\mathbf{x_M} = \mathbf{T^{-1}x}$, $\mathbf{B_M} = \mathbf{T^{-1}B}$, $\mathbf{C_M} = \mathbf{CT}$). The transformed system, denoted by the subscript $\mathbf{M}$, is more suitable for analysis. $\mathbf{A_M}$ is a diagonal matrix, turning explicit its eigenvalues, and enabling the decoupling of the original system in N second order subsystems formed by real or conjugate pairs of eigenvalues.

3.2 Modal Reduction

In this stage, we find which of the subsystems are most suitable to approximate the original model, by computing each subsystem's static gain. This approach relies on the largely dominance of a few eigenvalues on the system's response, since higher frequencies are very attenuated by hydrodynamical forces and the smoothness of the input.

The selected subsystems are combined in a reduced model ($\dot{\mathbf{z}} = \mathbf{A_R z} + \mathbf{B_R} u$, $y = \mathbf{C_R z} + \mathbf{D_R} u$), whose order is chosen considering the trade-off between the accuracy of the reduced dynamics and the simplicity of the control structure required. In addition, the reduced system must account for the static gain lost in the neglected eigenvalues. This is performed by the direct transfer matrix $\mathbf{D_R}$, which is the difference between the original and the reduced systems gains:

$$\mathbf{D_R} = \mathbf{CA^{-1}B} - \mathbf{C_R A_R^{-1} B_R} \tag{8}$$

The direct transfer matrix $\mathbf{D_R}$ introduces new dynamics: a non-zero output that does not take the propagation delay of the input into account, and a high frequencies gain. As shown in Fortaleza (2009), we can refine the reduced model introducing a input delay ϵ that minimizes the direct transfer and guarantees zero dynamics for $t < \epsilon$:

$$\begin{aligned} \dot{\mathbf{z}} &= \mathbf{A_R z} + \mathbf{B_D} u(t-\epsilon) \\ y &= \mathbf{C_R z} + \mathbf{D_D} u(t-\epsilon) \end{aligned} \tag{9}$$

with

$$\mathbf{B_D} = \mathbf{A_M}(e^{\epsilon \mathbf{A_M}})\mathbf{A_M^{-1}B_M} \tag{10}$$

$$\mathbf{D_D} = \mathbf{C_M}(e^{\epsilon \mathbf{A_M}} - \mathbf{I})\mathbf{A_M^{-1}B_M} + \mathbf{D_M} \tag{11}$$

The new reduced model (9) is so that for a step input at the instant t', the output keeps its initial value while $t < t' + \epsilon$. For $t \geq t' + \epsilon$, both reduced models produce the same output. The delay ϵ can be seen as an approximation for the natural propagation delay in the structure.

4. CONTROL DESIGN

4.1 Off-line Trajectory Planning

The dynamics of the reduced-order model (9) are compared with those of the original system. Choosing an reduction to order 4, with two pairs of complex conjugate eigenvalues (λ_i,$\overline{\lambda}_i$, with $\lambda_i = \sigma_i + jw_i$), the system's state space equation are

$$\begin{aligned} \begin{pmatrix} \dot{z}_1 \\ \dot{z}_2 \\ \dot{z}_3 \\ \dot{z}_4 \end{pmatrix} &= \begin{pmatrix} \sigma_1 & w_1 & 0 & 0 \\ -w_1 & \sigma_1 & 0 & 0 \\ 0 & 0 & \sigma_2 & w_2 \\ 0 & 0 & -w_2 & \sigma_2 \end{pmatrix} \begin{pmatrix} z_1 \\ z_2 \\ z_3 \\ z_4 \end{pmatrix} + \begin{pmatrix} b_1 \\ b_2 \\ b_3 \\ b_4 \end{pmatrix} u(t-\epsilon) \\ y &= (c_1 \;\; c_2 \;\; c_3 \;\; c_4) \begin{pmatrix} z_1 \\ z_2 \\ z_3 \\ z_4 \end{pmatrix} + (d)\, u(t-\epsilon) \end{aligned} \tag{12}$$

Normally the trajectory planning problem consists in finding an open-loop control $u^*(t)$ such that the system's state variables follow an arbitrary trajectory $\mathbf{z}^*(t)$. However, for the reduced model, $\mathbf{z}^*(t)$ lacks physical interpretation, i.e, does not have a clear relation to the riser's original state variables, and, therefore, to the reentry maneuver itself. A solution is dealing with the desired trajectory of the system's flat output.

We first compute Kalman's controllability matrix $\mathbf{K}$ for the system above ($\mathbf{K} = \begin{bmatrix}\mathbf{B} & \mathbf{AB} & \mathbf{A^2B} & \mathbf{A^3B}\end{bmatrix}$). As controllability is equivalent to flatness for linear systems, full rank is a sufficient condition for the system to be flat. The flat output is a linear combination of the state variables (z_1, z_2, z_3, z_4), obtained from the last row of the inverse of $\mathbf{K}$ (see Sira-Ramirez and Agrawal, 2004):

$$f = [0 \;\; 0 \;\; 0 \;\; 1]\, \mathbf{K^{-1}z} \tag{13}$$

$$f = \alpha_1 z_1 + \alpha_2 z_2 + \alpha_3 z_3 + \alpha_4 z_4 \tag{14}$$

The coefficients of the state variables in the equation above are omitted. The system order corresponds to the number of times the flat output f must be differentiated, to obtain an expression for the input u that depends on just f and its time derivatives. Differentiating f yields

$$\begin{aligned} \dot{f} &= \alpha_5 z_1 + \alpha_6 z_2 + \alpha_7 z_3 + \alpha_8 z_4 \\ \ddot{f} &= \alpha_9 z_1 + \alpha_{10} z_2 + \alpha_{11} z_3 + \alpha_{12} z_4 \\ f^{(3)} &= \alpha_{13} z_1 + \alpha_{14} z_2 + \alpha_{15} z_3 + \alpha_{16} z_4 \\ f^{(4)} &= \alpha_{17} z_1 + \alpha_{18} z_2 + \alpha_{19} z_3 + \alpha_{20} z_4 + \gamma u \end{aligned} \tag{15}$$

whose coefficients α_i are obtained by using the model equations (12) during the differentiation process. Equations (14) e (15) provide the coefficients for the matrix $\mathbf{M}$

$$\mathbf{M} = \begin{pmatrix} \alpha_1 & \alpha_2 & \alpha_3 & \alpha_4 & 0 \\ \alpha_5 & \alpha_6 & \alpha_7 & \alpha_8 & 0 \\ \alpha_9 & \alpha_{10} & \alpha_{11} & \alpha_{12} & 0 \\ \alpha_{13} & \alpha_{14} & \alpha_{15} & \alpha_{16} & 0 \\ \alpha_{17} & \alpha_{18} & \alpha_{19} & \alpha_{20} & \gamma \end{pmatrix} \tag{16}$$

so that

$$\begin{pmatrix} f \\ \dot{f} \\ \ddot{f} \\ f^{(3)} \\ f^{(4)} \end{pmatrix} = \mathbf{M} \begin{pmatrix} z_1 \\ z_2 \\ z_3 \\ z_4 \\ u \end{pmatrix} \tag{17}$$

from the last row of $\mathbf{M^{-1}}$, we finally obtain

$$u = \beta_0 f + \beta_1 \dot{f} + \beta_2 \ddot{f} + \beta_3 f^{(3)} + \beta_4 f^{(4)} \tag{18}$$

Equation (18) completely determines the input u in terms of the flat output f and its time derivatives. By choosing a desired trajectory $f^*(t)$, at least 4 times differentiable, that satisfies the initial and final conditions of the state vector $\mathbf{z}$ and the input u, it is trivial to find the desired open loop control $u^*(t)$.

The next step is planning the riser bottom trajectory using polynomial interpolation for $f^*(t)$:

$$f^*(t) = \begin{cases} 0, & \forall t < t' \\ \sum_{k=0}^{11} a_i t^k \\ c_f, & \forall t > t_f + t' \end{cases} \tag{19}$$

The coefficients a_i are found by imposing $f^*(t)$ zero at an arbitrary instant when the operation begins ($t = t'$) and a final value c_f after an operation time t_f ($t = t_f + t'$), according to the distance between the initial position of the riser and the wellhead location. The first five time derivatives of $f^*(t)$ are made null in both instants (hence the polynomial of order 11), assuring a smooth reference trajectory for $f^{(4)}$ in the vicinity of the final value c_f.

4.2 Trajectory Tracking

After the trajectory planning for the flat output, a natural step is the design of a feedback control law such that a trajectory error $e = f - f^*(t)$ is corrected. For every flat system, it is possible to compute an endogenous dynamic feedback, such that the system is equivalent to a trivial linear controllable system in Brunovsky's form. For more details, see Levine (2009).

With the following change in input coordinates

$$v = -\frac{\beta_0}{\beta_4} f - \frac{\beta_1}{\beta_4} \dot{f} - \frac{\beta_2}{\beta_4} \ddot{f} - \frac{\beta_3}{\beta_4} f^{(3)} + \frac{1}{\beta_4} u \tag{20}$$

the system described by (18) reads

$$v = f^{(4)} \tag{21}$$

A tracking feedback controller is made by setting

$$v = f^{*(4)} - k_4 e^{(3)} - k_3 \ddot{e} - k_2 \dot{e} - k_1 e - k_0 \int_0^t e \, dt \tag{22}$$

with the gains k_i chosen such that the closed-loop characteristic polynomial $s^5 + k_4 s^4 + k_3 s^3 + k_2 s^2 + k_1 s + k_0$ is stable (see Levine, 2009). Thus, as the error e exponentially converges to 0, f and its time derivatives up to the 4th order converge to their reference trajectories $f^*(t), \ldots, f^{*(4)}(t)$. In (22) the error integral term $-k_0 \int_0^t e \, dt$ is introduced to ensure static errors due to external perturbations, such as marine currents, are corrected.

The final expression for the original input u is given by

$$u = \beta_0 f + \beta_1 \dot{f} + \beta_2 \ddot{f} + \beta_3 f^{(3)} + \beta_4 v \tag{23}$$

with v given by (22).

A remaining problem is the on-line computing of the reduced model state variables based on the output of the real plant, i.e., the bottom end of the riser system during operation. For that a standard Kalman filter was implemented (Kalman, 1960). Fig. 2 shows the block diagram of the controlled plant:

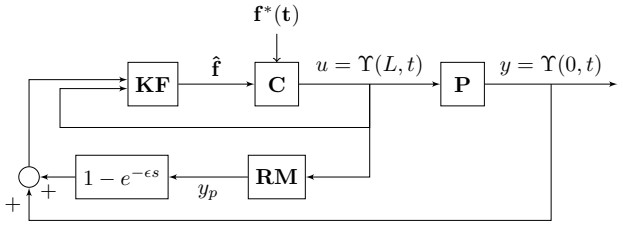

Fig. 2. Block diagram of the control structure

in which **P** denotes the actual plant, **C**, the controller developed in this section, whose inputs are the nominal precomputed trajectories $\mathbf{f}^*(\mathbf{t})$ and the estimated trajectories $\hat{\mathbf{f}}$ for the flat output and its time derivatives. **RM** is the reduced model (9), whose input is kept undelayed, resulting in a predictive internal model of the plant. This is used for the smith predictor structure seen in the outer loops of the diagram (see Ogata, 2001). The block **KF** denotes the Kalman filter, which estimates the state variables $\hat{\mathbf{z}}$, and computes $\hat{\mathbf{f}}$, through equations (14) and (15).

5. SIMULATION RESULTS

Numerical simulations were carried out to assess the performance of the trajectory planning and tracking tasks. Table 1 presents the parameters used for the structure. In addition, choosing a model order of 600 was proven enough to a good approximation of the original PDE (3) of the system, by comparing the frequency of the first and second vibration modes with their theoretical values.

For all simulations, a 4th order reduced model is considered. As a initial condition, both ends of the riser are stationary. Then, the payload is moved to a final position 1 m away, and both ends should be again stationary, as a final condition.

Fig. 3 provides three different plots. First, the nominal input, obtained by raw trajectory planning, replacing (19) in (18), since the error e is null for this case. Then, the response on the bottom end of the riser is plotted and compared to the ideal reference trajectory. Despite the order reduction and the hydrodynamic drag linearization used for the planning, the simulated structure presents low overshoot and oscillation around the final position.

The operation time t_f, chosen 130 s, is an important parameter: it determines the contribution of high frequency

Table 1. Parameters of the simulated structure

Parameter	Value
External Diameter	0.15 m
Internal Diameter	0.12 m
Length	2000 m
Steel Elastic Modulus	210×10^9 Pa
Steel Density	8.03×10^3 kg/m
Top boundary condition	Fixed end
Bottom boundary condition	Free end
Drag coefficient	1.2
Added mass coefficient	2.0
Payload mass	40×10^3 kg
Payload diameter	3 m
Payload Drag coefficient	0.7
Payload added mass coefficient	1.4

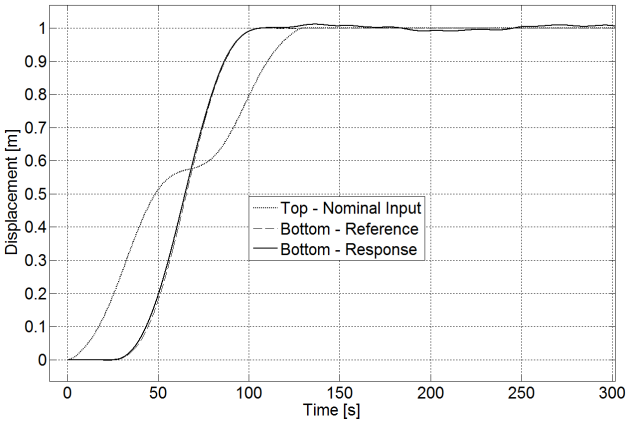

Fig. 3. Nominal trajectories for the riser's top and bottom ends and the actual bottom end response.

eigenvalues in the riser bottom end, which are left out of the reduced model. If t_f is too big, higher overshoot and oscillation are expected. Also, the top nominal input tends to a non-convex curve, which poses challenges to its feasibility. In this case, the latter is the limiting factor, as can be observed in Fig. 3 around $t = 60s$ with the required top input deceleration.

Fig. 4 compares the performance of pure trajectory planning against the robustness of the tracking system shown in 2, regarding a transient disturbance on the input. Besides the much faster error convergence achieved, the smith predictor plays a key role, since with a conventional controller, the bottom response would be highly impacted by the disturbance before any feedback control action could be taken. Instead, the disturbance is greatly softened during its first propagation on the structure.

As a disadvantage, the controller can't attenuate the high frequency disturbance generated by its own action, since it has a smaller period than the structure's propagation delay. Despite that, the achieved quality of the response can't be much affected, since those high frequencies always have small amplitude, due to the nonlinear nature of drag.

Marine current is introduced by modifying the hydrodynamic load (2):

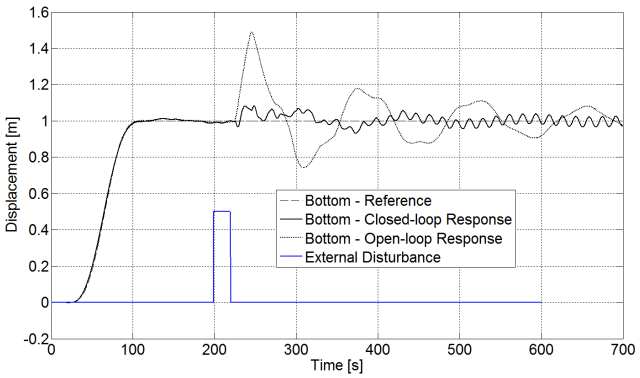

Fig. 4. Transient disturbance: open-loop and closed-loop bottom end response.

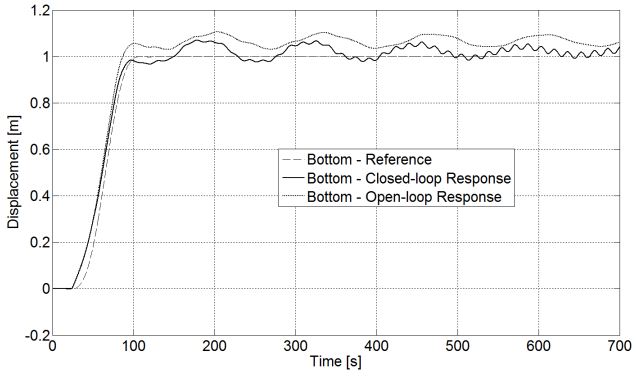

Fig. 5. Current disturbance: open-loop and closed-loop bottom end response.

$$F_n(z,t) = -m_f \frac{\partial^2 \Upsilon}{\partial t^2} - \mu \left| \frac{\partial \Upsilon}{\partial t} - U(z,t) \right| \left(\frac{\partial \Upsilon}{\partial t} - U(z,t) \right) \tag{24}$$

with $U(z,t)$ being the transversal fluid velocity along the riser's length.

Marine currents typically concentrate energy on low depths and generate a slow varying offset, which can be assumed constant during the reentry operation. Therefore, $U(z,t)$ is assigned 0.2 m/s for the first 100 meters and decreases linearly till 0 for the next 100 meters. Fig. 5 shows that the open-loop plant presents a small deviation from the nominal trajectory during the operation, but acquires steady-state error. This is corrected by the closed-loop controller.

For Fig. 6, a permanent sinusoidal disturbance is introduced in the input:

$$p(t) = 0.15 \sin(0.2\pi t) + 0.1 \cos(\pi t) \tag{25}$$

Initially, the controller doesn't show much improvement on the riser response. However, after around $t = 300$ seconds, significant attenuation on the main amplitude of the disturbance can be noticed.

6. CONCLUSION

The control design developed in this paper can be divided in three stages. First, an order reduction was applied to the

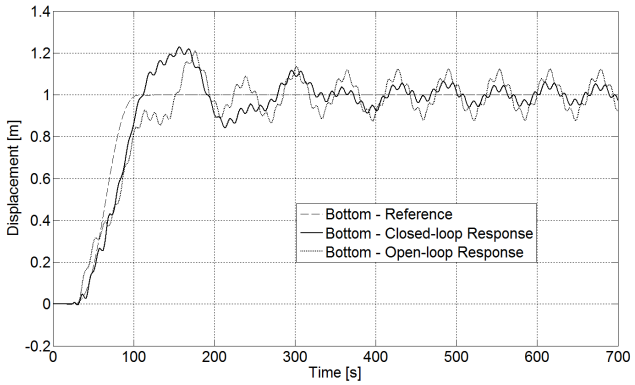

Fig. 6. Sinusoidal permanent disturbance: open-loop and closed-loop bottom end response.

discretized riser model, maintaining the dynamics of the most significant vibration modes of the structure. Second, the reduced model was used for trajectory planning with the flatness approach. At last, a closed-loop control law is proposed based on state estimation for the reduced model and predictive control to increase performance.

This approach does not require a high complexity control structure, analytical solutions or model inversion. Thus, it can be applied with more generality to other subsea distributed parameter systems. Numerical simulations illustrate the performance achieved for pure trajectory planning and for tracking in different situations.

In further studies, we expect to validate the controller with a didactic platform for a subsea riser.

REFERENCES

Dahleh, M.; Dahleh, M.V.G. (2011). Lectures on dynamic systems and control, chapter 12: Modal decomposition of state-space models. MIT OpenCourseWare.

Fortaleza, E. (2009). *Active Control Applied to Offshore Structures: Positioning and Attenuation of Vortex Induced Vibrations*. Ph.D. thesis, ECOLE NATIONALE SUPERIEURE DES MINES DE PARIS.

Fortaleza, E., Albuquerque, D., and Yamamoto, M. (2012). An investigation about the trajectory control during the subsea equipment installation using cable. In *ASME 2012 31st International Conference on Ocean, Offshore and Arctic Engineering*, 631–636. American Society of Mechanical Engineers.

Fortaleza, E., Creff, Y., and Lévine, J. (2011). Active control of a dynamically positioned vessel for the installation of subsea structures. *Mathematical and Computer Modelling of Dynamical Systems*, 17(1), 71–84.

Ioki, T., Ohtsubo, K., Kajiwara, H., Koterayama, W., Nakamura, M., et al. (2006). On vibration control of flexible pipes in ocean drilling system. In *The Sixteenth International Offshore and Polar Engineering Conference*. International Society of Offshore and Polar Engineers.

Kalman, R.E. (1960). A new approach to linear filtering and prediction problems. *Journal of Fluids Engineering*, 82(1), 35–45.

Levine, J. (2009). *Analysis and control of nonlinear systems: A flatness-based approach*. Springer.

Ogata, K. (2001). *Modern control engineering (4th edition)*. Prentice Hall.

Sabri, R. (2004). *Installation des Conduites Petrolires en Mer Profonde par Controle Actif*. Ph.D. thesis, ECOLE NATIONALE SUPERIEURE DES MINES DE PARIS.

Sira-Ramirez, H. and Agrawal, S.K. (2004). *Differentially flat systems*, volume 17. CRC Press.

Yamamoto, M., Morooka, C.K., and Ueno, S. (2007). Dynamic behavior of a semi-submersible platform coupled with drilling riser during re-entry operation in ultra-deep water. In *ASME 2007 26th International Conference on Offshore Mechanics and Arctic Engineering*, 239–248. American Society of Mechanical Engineers.

